AIIM

Association for Information and Image Management

1100 Wayne Avenue, Suite 1100
Silver Spring, Maryland 20910

301/587-8202

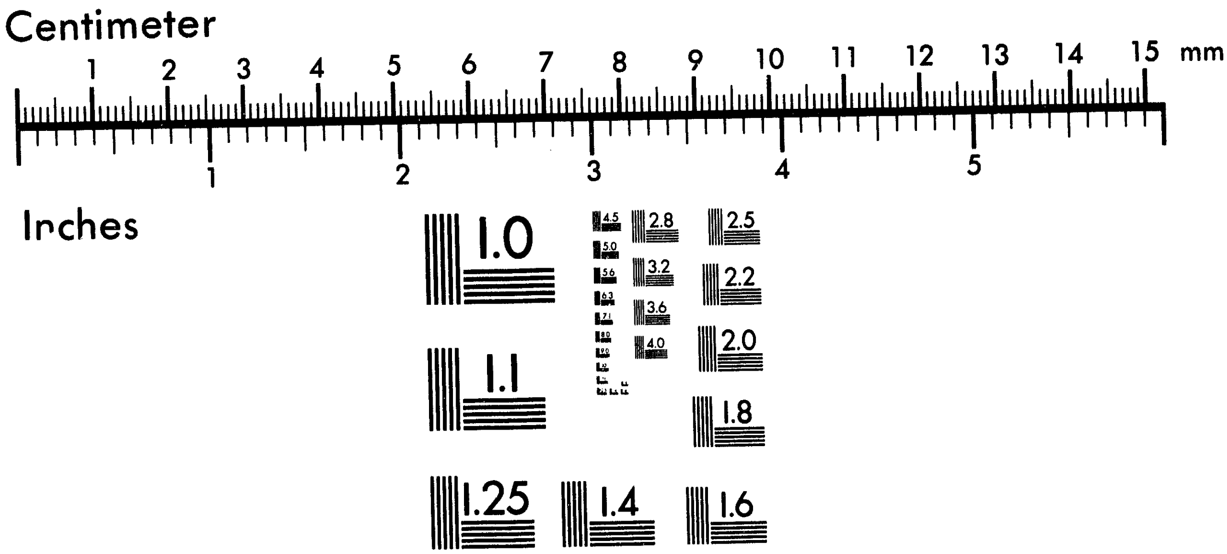

MANUFACTURED TO AIIM STANDARDS
BY APPLIED IMAGE, INC.

1 of 1

ANL/TD/CP--82096
CONF-940630--34

Plasma Disruption Modeling and Simulation*

A. Hassanein
Argonne National Laboratory
9700 South Cass Avenue
Argonne, Illinois 60439 USA

DISCLAIMER

June 1994

* Work supported by the United States Department of Energy, Office of Fusion Energy, under contract W-31-109-Eng-38.

An invited paper to be presented at the 11th Topical Meeting on the Technology of Fusion Energy, June 19 - 23, 1994, New Orleans, Louisiana.

PLASMA DISRUPTION MODELING AND SIMULATION*

A. Hassanein
Argonne National Laboratory
9700 South Cass Avenue, Bldg. 207
Argonne, IL 60439
(708) 252-5889

ABSTRACT

Disruptions in tokamak reactors are considered a limiting factor to successful operation and a reliable design. The behavior of plasma-facing components during a disruption is critical to the overall integrity of the reactor. Erosion of plasma facing-material (PFM) surfaces due to thermal energy dump during the disruption can severely limit the lifetime of these components and thus diminish the economic feasibility of the reactor. A comprehensive understanding of the interplay of various physical processes during a disruption is essential for determining component lifetime and potentially improving the performance of such components.

There are three principal stages in modeling the behavior of PFM during a disruption. Initially, the incident plasma particles will deposit their energy directly on the PFM surface, heating it to a very high temperature where ablation occurs. Models for plasma-material interactions have been developed and used to predict material thermal evolution during the disruption. Within a few microseconds after the start of the disruption, enough material is vaporized to intercept most of the incoming plasma particles. Models for plasma-vapor interactions are necessary to predict vapor cloud expansion and hydrodynamics. Continuous heating of the vapor cloud above the material surface by the incident plasma particles will excite, ionize, and cause vapor atoms to emit thermal radiation. Accurate models for radiation transport in the vapor are essential for calculating the net radiated flux to the material surface which determines the final erosion thickness and consequently component lifetime. A comprehensive model that takes into account various stages of plasma-material interaction has been developed and used to predict erosion rates during reactor disruption, as well during induced disruption in laboratory experiments. Differences between various simulation experiments and reactor conditions are discussed. A two-dimensional radiation transport model has been developed to particularly simulate the effect of small test samples used in laboratory disruption experiments.

*Work supported by the U.S. Department of Energy, Office of Fusion Energy, under Contract W-31-109-Eng-38.

I. INTRODUCTION

During disruptions, the plasma-facing material (PFM) of a tokamak reactor will be exposed to very high heat loads for short periods of time. A large fraction of the plasma thermal energy will be deposited on the PFM surface, resulting in very high surface temperature and subsequently very high thermal erosion of the PFM. Estimated energy densities of 10-200 MJ/m^2 will be deposited in a duration of 0.1-3 ms. The response of the PFM to such heat loads is critical to reactor operation and design. A comprehensive understanding of the interplay of various physical processes during plasma-material interaction is very important in determining component lifetime and in potentially improving component performance.

Previous analysis of this problem has focused on separate individual tasks related to plasma-facing interactions during the disruption.[1-10] However, there are three major stages for modeling material response during a disruption. Initially, the incident plasma particles from the disrupted plasma will deposit part of their energy on

the PFM surface. To predict the initial behavior of PFM, models are required for particle deposition and material thermal evolution; these models must take into account phase change, moving boundaries, and temperature-dependent thermophysical properties, etc. The initial burst of energy delivered to PFM surfaces from the direct impact of plasma particles will cause sudden ablation of the materials. As a result, a vapor cloud will be formed in front of the incoming plasma particles. Shortly thereafter, the plasma particles will be completely stopped in this vapor cloud. Comprehensive models for the hydrodynamics and heating of the vapor cloud that shields the original surface are then required for the second stage of disruption modeling. The continuous heating of the vapor cloud, therefore, will ionize, excite, and generate photon radiation. Thus, the initial plasma particle kinetic energy is transformed into radiation energy. Finally, models for radiation transport throughout the vapor cloud are required in order to estimate the net heat flux transmitted to the PFM. It is the dynamics and the evolution of this vapor cloud that will finally determine the net erosion rate at the end of a disruption.

Figure 1 is a schematic illustration of the various interaction zones and processes that occur during the plasma-material interaction following a disruption or simulation experiment. This problem involves three moving boundaries: the vapor front, the receding target surface, and the solid-liquid interface. These three moving boundaries are interdependent, and a complete solution should link them dynamically and simultaneously. A recently developed comprehensive model is used in this analysis to account for interplay of all physical processes during the plasma-material interaction.[11] Models for thermal evolution of a material, plasma-vapor interaction physics, vapor hydrodynamics, and two-dimensional radiation transport have been developed, integrated, and perfected in a self-consistent way in sufficient detail to realistically simulate the effect of a disruption on PFM. Candidate PFMs such as beryllium and carbon were considered in this analysis. The dependence of net erosion rate on the characteristics of plasma-vapor interaction zone was analyzed and discussed.

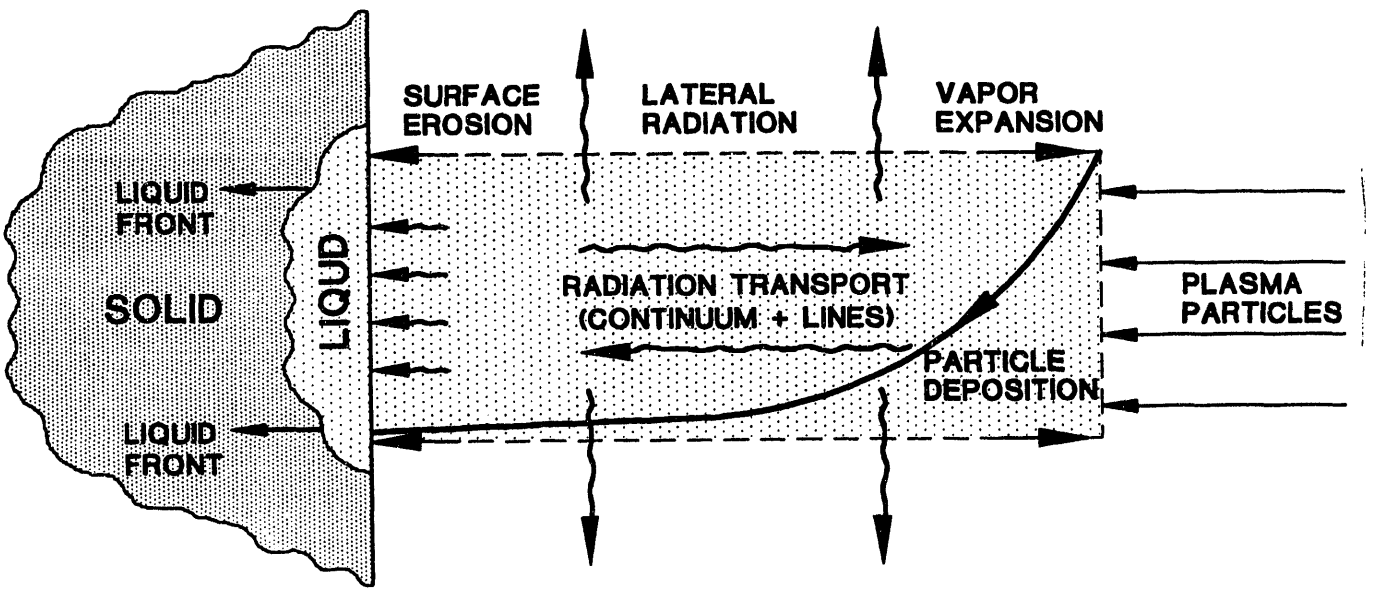

Fig. 1 Schematic illustration of various interaction zones and processes during a disruption.

II. SIMULATION EXPERIMENTS

Laboratory experiments to simulate plasma disruptions have been actively pursued with several reactor candidate materials and different high-intensity power sources. Among these sources are laser light, electron and ion beams, and plasma guns.[12-17] The majority of these experiments have relatively reactor-relevant disruption parameters (i.e., heat loads of 10-20 MJ/m^2 and deposition time of <1 ms). The erosion results from these experiments, however, do not agree. In particular, recent plasma gun experiments have yielded much lower erosion rates than in previous laser and electron beam experiments. One reason can be the very low particle kinetic energy used in the gun experiments ($E < 100$ eV). An attempt has been made to evaluate the key factors and differences among these experiments, including the effect of particle kinetic energy, particle type, beam momentum, and multidimensional effects of radiation transport. Because of the small size of the test samples, a two-dimensional multigroup radiation transport model (for both lines and continuum radiation) has been developed. In some disruption experiments and conditions, a large fraction of the incident energy is lost and radiated away from the specimen surface, resulting in lower erosion rates.

III. MODEL SUMMARY

A. Plasma-Material Interaction

The thermal response of PFM is calculated by solving a time-dependent heat conduction equation.[18] All thermophysical properties are assumed to be temperature-dependent. Plasma-particle (ions and electrons) energy deposition is calculated with detailed models that include elastic and inelastic slowing-down physics. Phase transformation of metallic plasma-facing components is taken into account in detail.[19] The incident plasma particle kinetic energy, photon energy radiated by the vapor cloud, vapor conducted energy, and free-streaming energy are partitioned inside the PFM into conduction, melting, and evaporation energy.[11]

B. Plasma-Vapor Interaction

The continuous deposition of plasma energy in the vapor cloud, which begins early in the disruption, will produce intense bulk vapor heating and vapor ionization. The vapor expansion into the vacuum chamber is determined by solving the vapor hydrodynamic equations for conservation of mass, momentum, and energy.[11] Both the incident plasma particle momentum and the effect of an existing magnetic field can be taken into account in this model.

C. Radiation Transport

After enough vapor accumulates in front of the incoming plasma particles, the plasma particles are then completely stopped in the vapor cloud, heating and ionizing it. Continuous deposition of incident plasma energy in the vapor will cause the vapor to radiate photons. The transport of these photons in the vapor layer is very important in determining the fraction of plasma energy transmitted to the PFM and subsequently determining the final erosion rate and lifetime of these components. It is then quite important to correctly model the radiation transport for a wide range of vapor conditions. For quasistationary conditions, the transport equation for the radiation has the form

$$\vec{\Omega} \nabla \vec{I}_\upsilon = \varepsilon_\upsilon - k_\upsilon \vec{I}_\upsilon , \qquad (1)$$

where $\vec{I}_\upsilon$ is radiation intensity, υ is frequency, ε_υ is vapor emissivity, $\vec{\Omega}$ is the solid angle, and k_υ is the absorption coefficient. Several methods are available for solving radiation transport equations. The most appropriate, however, is the so-called forward-reverse method.[20] This method is more appropriate in treating and describing both optically thick and optically thin plasma conditions. Other popular methods, such as diffusion approximation are valid only for optically thick plasma and should not be where the vapor is optically thin, particularly for low-Z PFM. The forward-reverse method treats the photon flux moving to the right (forward) I_υ^+ separately from the photon flux moving to the left (reverse) I_υ^-. For simplicity, in the one-dimensional (1-D) case the radiation fluxes in the forward and reverse direction are calculated for each vapor zone as

$$\frac{1}{2}\frac{d\, I_\upsilon^\pm}{d\, r} = \varepsilon_\upsilon - I_\upsilon^\pm , \qquad (2)$$

where r is the perpendicular distance in the vapor zone above the surface. In the two-dimensional (2-D) case, the magnitudes of the forward and reverse photon fluxes for each vapor zone are controlled by the solid angle sustained by the exposed disrupted area and the distance from this area to this vapor zone. Lateral escaping radiation fluxes can be quite high and can affect both vapor hydrodynamics and the resulting erosion rates.

In these calculations, the radiation fluxes are composed of two separate components, the continuum radiation flux I_{c_υ} and lines radiation flux I_{ℓ_υ}, so that

$$I_\upsilon^{\pm} = I_{c\upsilon}^{\pm} + I_{\ell\upsilon}^{\pm} . \qquad (3)$$

Therefore, the most intense lines are treated separately using the Collisional Radiative Equilibrium (CRE) method. A set of rate equations is solved for the populations of each individual atomic level. The less intense lines are combined with the continuum radiation. The most intense lines are usually <100 lines for each of the beryllium and carbon materials. Each line is approximated by about 10-20 photon energy groups, depending on line shape and width. Doppler and Stark broadening of the lines of radiation are taken into account as a function of vapor temperature and density for each vapor zone. Multigroup approximations (1000-4000 photon groups) were used for the continuum solution of the above equations. Plank averaging was used for the optically thin regions, whereas Rosseland averaging was more preferred for the optically thick regions.[21] Opacity and emissivity data are provided in the form of tables for a wide range of expected vapor densities and temperatures.

IV ANALYSIS

The models summarized above, including the 2-D radiation transport model are implemented in a new version of the Computer Code A*THERMAL-S.[11] The thermal quench time during a reactor disruption or a simulation experiment is assumed in this analysis to be 100 μs. The calculations for the radiation transport and vapor hydrodynamics are extended up to 10 μs longer than the disruption time to simulate a real situation in which the vapor and the radiation flux cannot disappear immediately after the disruption. Disruption energy density of about 10 MJ/m^2 is used in this analysis. The effect of higher energy densities on erosion rates is analyzed elsewhere.[11] The analysis in this study is intended to show the effect of particle kinetic energy, the importance of line radiations, the 2-D effects of radiation transport, and the effect of large beam momentum in some simulation experiments on the erosion rate of candidate materials such as carbon and beryllium. In the 2-D calculations, the diameter of the disrupted area is assumed to be 2 cm, a typical size for disruption simulation experiments.

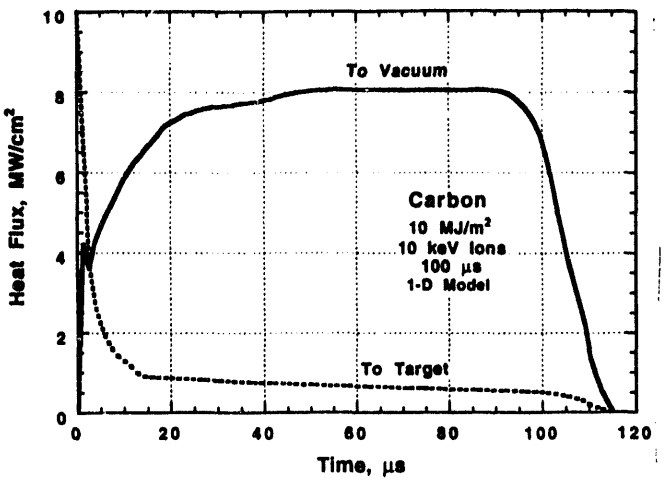

Fig. 2 Heat flux to target and to vacuum chamber.

Figure 2 shows the forward (to vacuum) and reverse (to target) heat flux from 10 keV plasma ions incident on carbon. Initially, the heat flux to the divertor or to the target material is equal to the incident heat flux due to direct deposition by the plasma particles. Shortly after the start of disruption, the heat flux to the target material decreases sharply due to the shielding and attenuation by the ablated material. After the plasma ions have completely stopped in the vapor, heating of the target material is mainly from vapor radiation. About 80% of the incident energy is radiated away from the disruption area, less than 10% is used to further heat the facing material, and the remainder is energy contained in the vapor material. The vapor cloud then significantly shields the exposed surface material from the original incident energy flux.

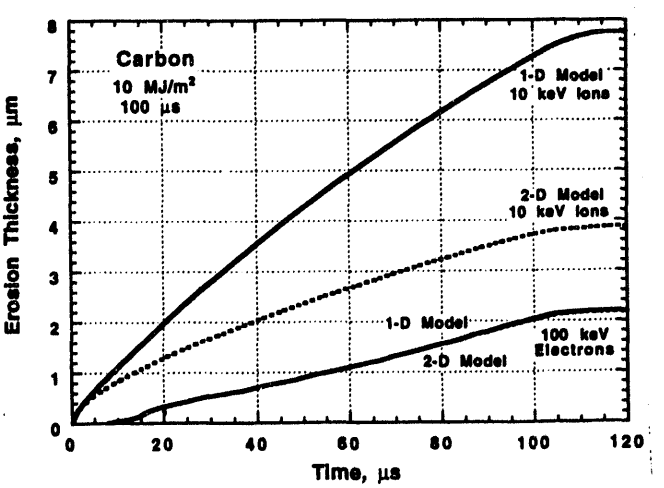

Fig. 3 Effect of particle type and energy on carbon erosion rate.

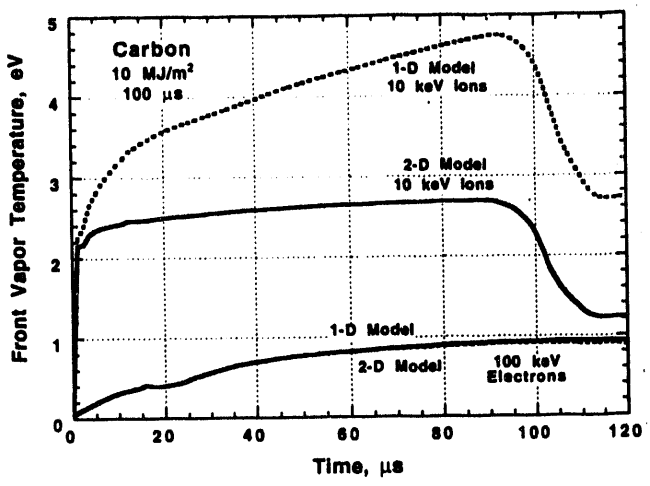

Fig. 4 Front carbon vapor temperature for different particle types and kinetic energies.

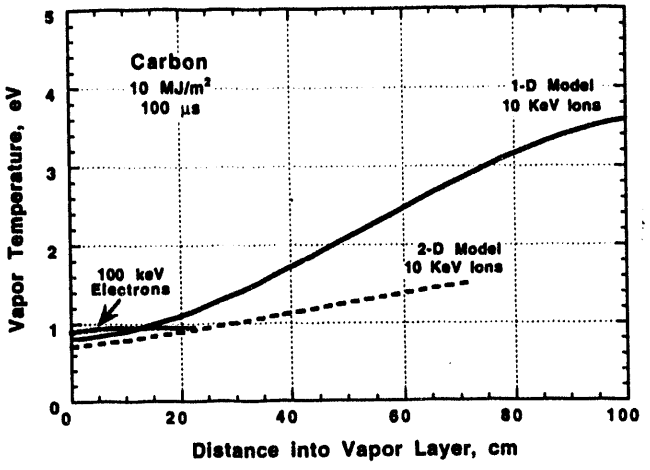

Fig. 5 Relationship of carbon vapor temperature to distance into vapor layer.

Figure 3 shows carbon erosion rates from 10 keV ions and 100 keV electrons calculated by both the 1- and 2-D models. The 100 keV electrons case is used because of the relevancy to disruption-simulation experiments with high-energy electron beams. The 10 keV ions case is more relevant to a reactor condition. The plasma ions usually have much shorter range in the PFM than do electrons with the same kinetic energy. Shorter range usually means higher surface temperature and thus higher erosion rate. Shorter range in the PFM also means shorter range in the developed vapor material, which means heating the front vapor zone to higher temperatures. Higher vapor temperature, in turn, usually means fast vapor expansion and high radiation fluxes. Both of these factors help substantiate 2-D lateral radiation losses that tend to reduce the net erosion rate, as shown in Fig. 3. However, for the 100 keV electrons, energy deposition inside the PFM is extended over a large mass and the resulting surface temperature in this case is much lower than in the ion case. This will result in a much lower erosion rate. Because the high-energy electrons will also have a long range in the vaporized material, the electrons will not heat the vapor to high temperature, as shown in Fig. 4. Therefore, the vapor will not have enough energy to emit substantial photon radiation. This is the main reason that the erosion rate for the electrons is practically the same in both the 1- and 2-D cases. The vapor front temperature in this case remains below 1 eV, resulting in a very low emitted radiation flux.

Figure 5 shows the relationship of carbon vapor temperature to distance into the vapor layer above the PFM surface. The higher the vapor temperature, the farther it expands away from the material surface. Again, because of the lower vapor temperature (< 1 eV) in the case of high-energy electron disruption, the carbon vapor only expands to about 20 cm above the surface. Because of escaping lateral radiations in the 2-D model for ions, the vapor temperature is reduced and so is vapor expansion above the surface.

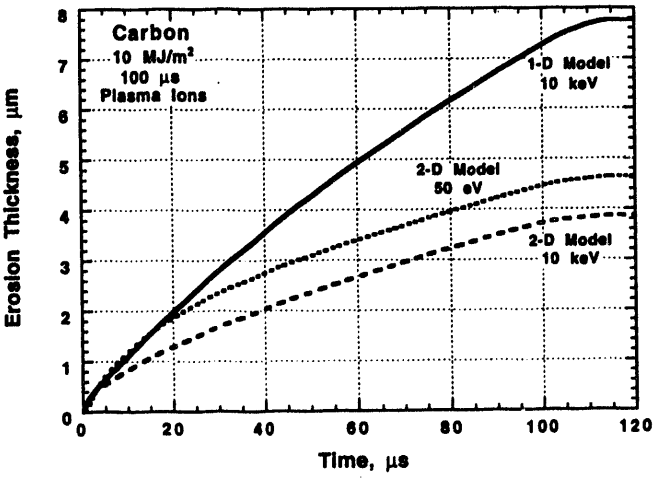

Fig. 6 Effect of low-energy plasma with high momentum on carbon erosion rate.

Plasma gun experiments used to simulate disruption have mainly used low-energy hydrogen ions (E < 100 eV). For the same energy density, plasma guns will have high particle momentum (tens of atmospheres). Figure 6

shows the effect of low-energy, high-momentum, plasma gun disruption simulation on carbon erosion rate. Ideally, the high plasma pressure associated with the plasma gun will confine the ablated material closer to the surface, thus reducing 2-D radiation losses, therefore, increasing the erosion rate. However, many uncertainties are associated with plasma gun experiments, including low particle-energy reflection, plasma source radiation, and high Z-impurities, that make modeling of such experiments extremely difficult.[22] Nevertheless, these results are in good agreement with recent plasma gun simulation experiments.[16]

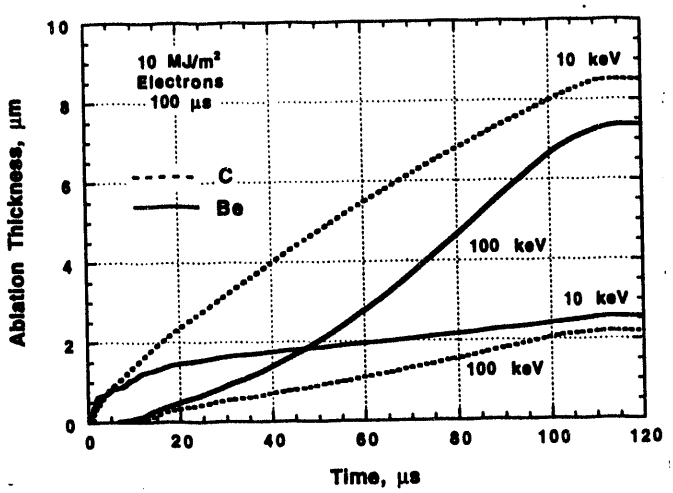

Fig. 7 Beryllium and carbon ablation thickness at different electron kinetic energies.

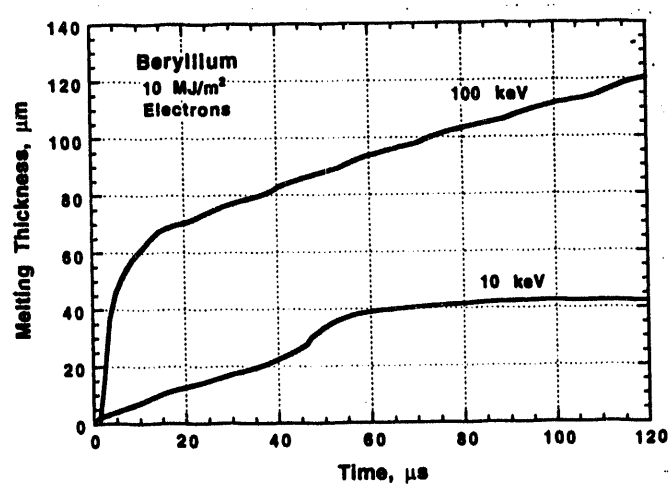

Fig. 8 Beryllium melt layer thickness for different electron kinetic energies.

Figure 7 compares beryllium and carbon erosion rates for electron kinetic energies of 10 and 100 keV. At the lower electron kinetic energy, the higher energy density deposited near PFM surface causes rapid vaporization. Incident energy is then deposited in the front vapor zone heating it to high temperatures. For beryllium, most of the radiation is emitted away from the PFM surface near the high-temperature zone, while for carbon, with its higher Z, more radiation is emitted and a higher fraction is directed toward the PFM surface resulting in more net erosion.[11] At higher electron kinetic energy, more energy is initially deposited deep inside the PFM, resulting in lower surface temperature and lower initial erosion rates. However, because of beryllium's higher thermal conductivity, more heat is then diffused from the bulk to the surface, causing significant erosion and melting as shown in Fig. 8. This may explain the high erosion rates of metallic targets in high-energy electron-beam simulation experiments.[13] Loss of the resulting thick melt layers from various forces during the experiments can significantly contribute to such high erosion rates.[23]

Laser beam simulation experiments usually produce higher erosion rates from vaporization, mainly because vapor shielding is significantly less important in these experiments.[12] Because of the very small size of the laser beam (diameter ≈1 mm), the beam penetrates through the expanded vapor cloud basically unattenuated, thus delivering most of its energy to the target material.

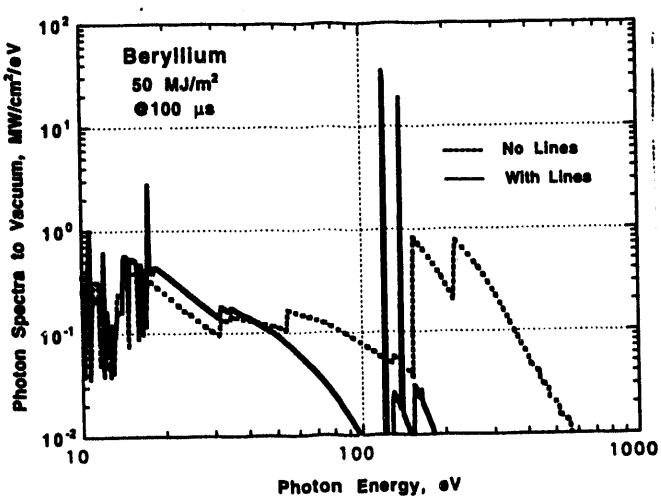

Fig. 9 Photon radiation spectra with and without lines of radiation.

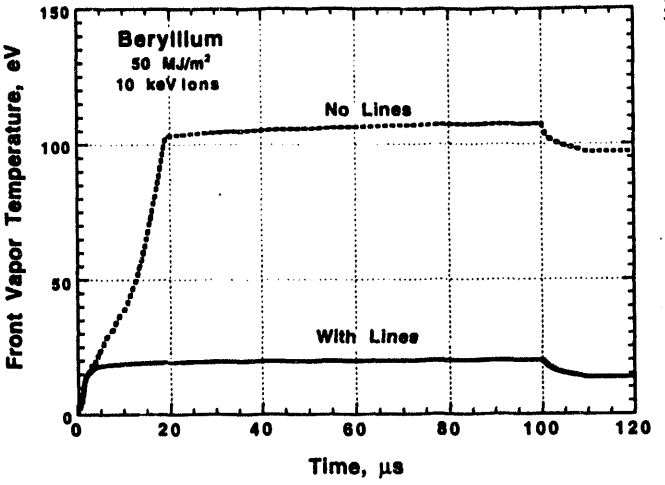

Fig. 10 Effect of lines of radiation on beryllium front vapor temperature.

Lines radiation in the vapor are particularly important for the low-Z and high-temperature vapor cloud. In most beryllium vapor cases, more than 90% of radiation from the front vapor zone is attributed to lines radiation. Figure 9 shows the calculated photon spectrum with and without lines of photons radiated from a beryllium vapor during a 50 MJ/m^2 disruption energy density. Excluding lines radiation result in significant overestimation of the continuum radiation spectrum. Figure 10 shows that excluding lines radiation can result in very high vapor temperatures that can significantly affect plasma-vapor interaction and vapor hydrodynamics. However, excluding lines radiation has less impact on the resulting overall erosion rate in this case.

Further analysis is needed for a number of important issues related to modeling of erosion depth during a disruption. One issue is the effect of an oblique magnetic field on the hydrodynamics of the vapor cloud that develops during a reactor disruption. A 2-D model was developed to study such an effect on the net erosion rate; preliminary analysis indicates that the magnetic field may reduce the overall erosion rate.[24] Another issue requiring investigation is the effect of a mixing zone between the incident plasma particles and the front vapor cloud. This zone can alter the radiative properties of the vapor zone, thus affecting net radiative heat flux to the PFM. This is important for both reactor disruption and simulation experiments.

Vapor thermal conduction with turbulence and vapor instabilities may significantly increase heat flux to the PFM, resulting in a substantial increase in erosion rate. Erosion of melt layers that develop during a disruption also requires further analysis and study. Loss of the melt layer can severely shorten divertor plate lifetime.

V. CONCLUSIONS

Various aspects of plasma disruption and simulation physics have been studied with a comprehensive dynamic model that integrates with fine detail and self-consistency, the material thermal evolution, plasma-vapor interaction physics, vapor hydrodynamics, and radiation transport. For accurate erosion-rate calculations for both reactor conditions and simulation experiments, one must take into account two-dimensional radiation transport, incident beam momentum, existence of magnetic fields, lines of radiation, and losses from melt layers developed during disruption of metallic plasma-facing components.

REFERENCES

1. A. Sestero and A. Ventura, J. Nucl. Mater. 128 & 129 (1984) 828.

2. A. Hassanein et al., Nucl. Eng. Design/Fusion 1 (1984) 307.

3. B.J. Merrill and J.L. Jones, J. Nucl. Mater. 111 & 112 (1982) 544.

4. H. Bolt et al., J. Nucl. Mater. 196-198 (1992) 948.

5. A. Hassanein and D. Ehst, J. Nucl. Mater. 196-198 (1992) 680.

6. B. Goel et al., Fusion Technology (1992) 272.

7. W. Höbel et al., J. Nucl. Mater. 196-198 (1992) 537.

8. R.R. Peterson, Radiative heat transfer in self-shielding vapor layer during tokamak disruptions, University of Wisconsin Report, UWFDM-357 (1983).

9. A. Hassanein and D. Ehst, J. Nucl. Mater. (1994).

10. J. Gilligan and D. Hahn, J. Nucl. Mater. 145-147 (1987) 391.

11. A. Hassanein and I. Konkashbaev, "Comprehensive Model for Disruption Erosion in a Reactor Environment," presented at 11th Intl. Conf. on Plasma-Surface Interactions, Mito, Japan, May 22-27, 1994. To be published in J. Nucl. Mater.

12. J.G. Van der Laan et al., J. Nucl. Mater. 196-198 (1992) 612.

13. J. Linke et al., J. Nucl. Mater. 196-198 (1992) 607.

14. M. Akiba et al., J. Nucl. Mater. 191-194 (1992) 373.

15. V.R. Barabash et al., J. Nucl. Mater. 187 (1992) 298.

16. J. Gahl et al., J. Nucl. Mater. 191-194 (1992) 454.

17. M. Bourham and J. Gilligan, 15th IEEE/NPSS Symp. on Fusion Engineering, Vol. I (1994) 23.

18. A. Hassanein, J. Nucl. Mater. 122 & 123 (1984) 1453.

19. A. Hassanein, ASME, 88-WA/NE-2.

20. B.N. Chetverushkin, Mathematical modelling of the radiative gas, Nauka, Moscow (1986).

21. I.V. Nemchinov, "The Averaging of the Radiation Transport Equations for the Radiation Transport in Gas," VINITI, N1721-83, Moscow, 1983.

22. A. Hassanein et al., accepted for publication in J. Nuclear Mater., March 1994.

23. A. Hassanein, Fusion Technology 15 (1989) 513.

24. A. Hassanein and I. Konkashbaev, "An Assessment of Disruption Erosion in ITER Environment," to be presented at 3rd Intl. Symp. on Fusion Nuclear Technology (ISFNT-3), Los Angeles, CA, June 27 - July 1, 1994.

DATE
FILMED
8/25/94
END